Differences in Structural, Textural, and Catalytic Properties of Montmorillonite Pillared with ($GaAl_{12}$) and ($AlAl_{12}$) Polyoxycations

M. J. Hernando, C. Pesquera, C. Blanco, I. Benito, and F. González*

Department of Chemistry, University of Cantabria, 39005 Santander, Spain

Received May 23, 1995. Revised Manuscript Received October 5, 1995[⊗]

This paper reports the preparation of a pillared montmorillonite using the mixed oligomer $[GaO_4Al_{12}(OH)_{24}(H_2O)_{12}]^{7+}$. Pillaring was performed with a starting solution having a molar ratio of $Al^{3+}/Ga^{3+} = 12$, which is equivalent to the stoichiometric ratio of this polyoxycation. To determine the optimum conditions for obtaining the desired product, we varied the $OH^-/(Al^{3+} + Ga^{3+})$ molar ratio in the range 1.5−2.5, which also produced variations in the pH of the oligomeric solution. The most favorable conditions were found to be $OH^-/(Al^{3+} + Ga^{3+}) = 2.0$ and pH = 3.7. The presence of mixed polyoxycations in the pillars of the synthesized materials was confirmed by NMR studies. The thermal stability and catalytic behavior of these materials in the hydrocracking and hydroisomerization of *n*-heptane have been compared with those of the material obtained from the same montmorillonite by pillaring with the $[AlO_4Al_{12}(OH)_{24}(H_2O)_{12}]^{7+}$ polyoxycation. The structure of the material pillared with the mixed polyoxycation shows higher thermal stability and retains 65% of its generated microporosity, up to 700 °C. This material also has greater stability in the number and strength of the Lewis acid sites of its pillars, resulting in higher selectivity for the isomerization of *n*-heptane.

Introduction

Pillared montmorillonites are smectite clay minerals that have been modified by introducing large polyoxycations into their interlayer regions. The intercalated cations are suitably chosen species capable of preventing the collapse of the interlayer spaces. Heating these materials results in the formation of inorganic oxide clusters that prop open the clay layers permanently, generating a microporous structure with a high specific surface area. The resulting material is of great interest because of its potential applications in various fields.[1]

The pillared laminar silicates obtained by intercalating inorganic polyoxycations (e.g., Al, Cr, Zr, ...),[2−8] including those pillared with the polyoxycation $[AlO_4Al_{12}(OH)_{24}(H_2O)_{12}]^{7+}$ (called the keggin ion), have been the most studied.

To prevent the clay layers from sintering, the thermal resistance of the pillars must be increased. One way of achieving this end, which has been tried by a number of authors[9−12] is to use mixed pillars. The existence of Al−Ga mixed polyoxycations, has been reported in the study of the hydrolisis of Ga^{3+} and Al^{3+} salts. This made it possible to prepare oligomer species in solution with a structure similar to that of the keggin ion but with the Ga^{3+} ion replacing the Al^{3+} ion in the central tetrahedral position,[13,14] $[GaO_4Al_{12}(OH)_{24}(H_2O)_{12}]^{7+}$. Later, the preparation of pillared clays using this oligomer was described by Bradley[15] and Poncelet.[16] We showed that the materials obtained in this way have greater thermal and hydrothermal stability.[17,18]

In these previous studies, we prepared the oligomeric solutions with different Al/Ga proportions but always in the range Al/Ga ≤ 3, and with a molar ratio of OH/Al + Ga = 2.0. It was found that the results became better when the Al^{3+}/Ga^{3+} molar ratio was increased. Taking these results into account, in the present study we decided to use a mixed oligomer with the molar ratio of Al/Ga = 12, which corresponds to the stoichiometric ratio of the $[GaO_4Al_{12}(OH)_{24}(H_2O)_{12}]^{7+}$ ion, which will be denoted by ($GaAl_{12}$). Keeping the molar ratio constant at this value, considered to be optimal, we have studied the influence of varying the OH/(Al + Ga) molar ratio from 1.5 to 2.5 on the properties of the resulting materials. The characteristics of the pillared materials obtained in this way have been compared with the materials obtained previously using lower proportions of Al/Ga.[18]

[⊗] Abstract published in *Advance ACS Abstracts,* November 15, 1995.

(1) Mitchell, I. V. *Pillared layered structures, current trends and applications*; Elsevier Applied Science: London, 1990.
(2) Figueras, F. *Catal. Rev.-Sci. Eng.* **1988**, *30*, 457.
(3) Tichit, D.; Fajula, F.; Figueras, F.; Ducouraut, B.; Mascherpa, G.; Gueguen, D.; Bousquet, J. *Clays Clay Miner.* **1988**, *36*, 369.
(4) Martín-Luengo, M. A.; Martins-Carvalho, H.; Ladriere, J.; Grange, P. *Clay Miner.* **1989**, *24*, 495.
(5) Figueras, F.; Martrod-Bashi, A.; Fetter, G.; Therier, A.; Zanchettr, J. V. *J. Catal.* **1986**, *34*, 658.
(6) Choudary, B. M.; Valli, V. I. K. *J. Chem. Soc., Chem. Commun.* **1990**, 1115.
(7) Shabtai, J.; Rosell, M.; Tokarz, M. *Clays Clay Miner.* **1984**, *32*, 99.
(8) Carrado, K. A.; Suib, S. L.; Skoularikis, N. D.; Coughlin, R. W. *Inorg. Chem.* **1986**, *25*, 4217.
(9) Occelli, M. L. *J. Mol. Catal.* **1986**, *35*, 377.
(10) Lee, W. L.; Tatarchuck, *J. Hyperfine Interact.* **1988**, *41*, 661.
(11) Sterte, J. *Clays Clay Miner.* **1991**, *39*, 167.
(12) Tang, X.; Shu, W. Q.; Shen, Y. F.; Suib, S. L. *Chem. Mater.* **1995**, *7*, 102.
(13) Bradley, S. M.; Kydd, R. A.; Yamdagni, J. *J. Chem. Soc., Dalton Trans.* **1990**, *2*, 413.
(14) Bradley, S. M.; Kydd, R. A.; Yamdagni, R. *Magn. Reson. Chem.* **1990**, *28*, 746.
(15) Bradley, S. M.; Kydd, R. A. *Catal. Lett.* **1991**, *8*, 185.
(16) Vieira, A.; Poncelet, G. *Appl. Catal.* **1991**, *77*, 303.
(17) González, F.; Pesquera, C.; Benito, I.; Mendioroz, S. *J. Chem. Soc., Chem. Commun.* **1991**, *8*, 587.
(18) González, F.; Pesquera, C.; Blanco, C.; Benito, I.; Mendioroz, S. *Inorg. Chem.* **1992**, *31*, 727.

0897-4756/96/2808-0076$12.00/0

Once it had been determined which sample pillared with ($GaAl_{12}$) had the best characteristics, we compared its properties with those of the sample pillared with the keggin ion $[AlO_4Al_{12}(OH)_{24}(H_2O)_{12}]^{7+}$, which will be denoted by ($AlAl_{12}$). First, the structural characteristics have been analyzed by NMR, giving evidence of the existence of mixed pillars ($GaAl_{12}$), consistent with experiments performed by TG and DRX. The texture of both materials has also been analyzed, paying special attention to the generation of microporosity and its thermal evolution and to the catalytic activity in hydrocracking and hydroisomerization of *n*-heptane.

Experimental Section

Starting Material. The clay used as the raw material is a bentonite from Serrata de Nijar (Almeria, Spain), supplied by Minas Gador S.A. Analysis of its mineralogic composition showed it to be 95% montmorillonite. Its structural formula, which was determined previously,[19] is as follows:

$$(Si_{7.95}Al_{0.05})(Al_{2.69}Fe_{0.32}Mg_{0.97})O_{20}(OH)_4(Ca_{0.13}Mg_{0.26}Na_{0.23}K_{0.02})$$

The raw clay was purified by fractionated sedimentation with the fraction <2 μm being collected. By means of cation exchange using a 1 M solution of NaCl we obtained homoionic montmorillonite which was washed until the Cl^- ion was eliminated. The sample obtained in this way had a surface area of 87 m^2/g and a pore volume of 0.084 cm^3/g, at $P/P_0 = 0.98$. Its exchange capacity was 59 mequiv/100 g of clay, and its basal spacing was 15.4 Å, which decreased to 9.9 Å at 500 °C.

Synthesis. *Preparation of the Pillaring Agent*. The solutions of ($GaAl_{12}$) polyoxycation were prepared by starting with 0.2 M solutions of $AlCl_3 \cdot 6H_2O + GaCl_3$, with an Al/Ga ratio of 12/1 and gradually adding appropriate volumes of 0.5 M NaOH solution to obtain different OH/(Al + Ga) ratios ranging from 1.5 to 2.5. The reaction mixture was then diluted with the quantity of water necessary to yield a 1M concentration of ($Al^{3+} + Ga^{3+}$). The solutions obtained in this way were refluxed for 24 h.

Pillaring Process. The solutions of pillaring agent were added with vigorous stirring to a clay slurry of 2.5 g/100 mL. The final proportion in all cases was 20 mequiv of (Al + Ga)/g of clay, with a solid/liquid ratio of 0.5%. The reaction mixture was stirred continuously for 24 h at room temperature. It was then washed by means of dialysis with distilled water, using 1 L of water/g of clay. Dialysis was continued with water being renewed every 24 h until the Cl^- ion concentrations decreased to the point where the conductivity of the washed water was <30 μS. Finally, the samples were freeze-dried.

Equipment and Methods. The following equipment and techniques were used for the physicochemical characterization of the materials:

Chemical Analysis was carried out by atomic absorption spectrometry with a Perkin-Elmer 560 instrument.

X-ray diffraction diagrams were determined using powder with the particles oriented so as to increase the intensity of the 001 reflection by means of a Philips PW-1710 diffractometer with Cu Kα radiation.

Thermal treatment involved subjecting the samples to temperatures of 500, 600, 700, and 800 °C for 2 h in a fixed-bed reactor with a flow of 100 cm^3/min of dry air.

Thermal analysis was performed in a Setaram TG-DSC 111 apparatus, with an air flow of 20 cm^3/g and a heating rate of 5°C/min.

IR Spectroscopy Acidity Study. Infrared spectra were obtained with a single-beam Perkin-Elmer Model 1605 FT-IR spectrophotometer, with a sensitivity of $\pm 4 cm^{-1}$ in the 1700−1300 cm^{-1} range and ±1% in transmittance. Self-supporting wafers were prepared by pressing ca. 25 mg of sample on an 18-mm-diameter die. The wafer was degassed by heating at 400 °C for 2 h in vacuo before performing pyridine adsorption on the sample for 30 min. Infrared spectra were recorded after evacuation at room temperature and heating for 2 h at various other temperatures from 100 to 400 °C.

Determination of Textural Parameters. The adsorption−desorption isotherm of N_2 at 77 K was determined in a Micromeritics ASAP 2000 with a micropore system. Specific surface was determined by applying the BET equation to the isotherm.[20] The total pore volume was considered to be the volume of N_2 liquid adsorbed at a relative pressure of 0.98. Microporosity was deduced by several methods: the *t*-plot of de Boer;[21] D−R of Dubinin−Radushkevitch;[22] and Horvath−Kawazoe (H−K) method.[23] The estimate obtained with the second method will include a certain amount of mesopore volume due to the deviation of the curve of the proposed equation at high values of P/P_0.[24] The H−K method gives the accumulative volume of pores smaller than 10 Å.

NMR Spectra. Magic-angle spinning nuclear magnetic resonance (MAS NMR) measurements were recorded on a Bruker AMX 300 spectrometer equipped with a multinuclear probe. Powder samples were packed in zirconia rotors. ^{29}Si spectra were obtained at 59.60 MHz, employing a pulse width of 4 μS, spinning rate of 4.0 kHz, spectra width of 20 kHz, recycle delay of 0.5 s, 12 000 scans, and 20-Hz exponential line broadening. Chemical shifts are reported in ppm from tetramethylsilane. ^{27}Al spectra were recorded at 78.23 MHz using a pulse width of 4 μs, spinning rate of 3.0 kHz, a spectral width of 50 kHz, a recycle delay of 0.3 s, 6000 scans, and 10-Hz exponential line broadening. Chemical shifts are reported in ppm from 0.1 M $[Al(H_2O)_6]^{3+}$.

Catalytic Activity. The pillared clays impregnated with Pt were used in the hydroisomerization−hydrocracking of *n*-heptane. This process gives a good evaluation of the strength of the acid sites. Two types of products can be obtained: products of isomerization and of cracking. In these bifunctional catalysts, the main role of the Pt is to dehydrogenate the alkane, which is then isomerized or cracked on the acid sites. The samples were impregnated with a 1% (w/w) ammoniacal complex of Pt. All samples were heated at 400 °C for 2 h under an air flow of 10 cm^3/min and then reduced in a flow of H_2 at 400 °C for 2 h. The catalytic reactions were carried out in a continuous flow system at a pressure of 1.0 atm with a fixed bed of 200 mg of catalyst under a constant flow of 10 cm^3/min of H_2 saturated with *n*-heptane at 27 °C. The WHSV (weight hour space velocity) was 0.9 g of *n*-heptane (g of catalyst h)$^{-1}$. The reaction was performed under temperature-programmed conditions using a heating rate of 1 °C/min, and reaction samples were collected every 25 °C. The products were analyzed in a Varian 3300 gas chromatograph using TCD with a Teknokroma column 9 m long × $^1/_8$ in. with SP1700 and 80/100 paw.

Results

Table 1 shows the different variables considered in the preparation of the samples. The file corresponding to each sample indicates the following data: denomination of the sample; molar ratios of Al^{3+}/Ga^{3+} and of OH/(Al + Ga) used in the preparation of the oligomer; pH of the oligomer after ageing; amount of Al^{3+} and Ga^{3+} cation incorporated (uptake) in mequiv/g; ratio of Al/Ga incorporated into the pillared product; and the number of pillars per gram of clay, assuming that each pillar corresponds to one ($GaAl_{12}$), or ($AlAl_{12}$) keggin cation.[14,25] Samples F and G are included in the table for the sake of comparison. Sample F shows the

(19) Pesquera, C. Thesis, University of Oviedo, 1989.

(20) Brunauer, S.; Emmett, P. H.; Teller, E. *J. Am. Chem. Soc.* **1938**, *60*, 309.
(21) deBoer, J. H. *J. Catal.* **1964**, 268.
(22) Dubinin, M. *Carbon* **1983**, *21*, 359.
(23) Horvath, G.; Kawazoe, K. *J. Chem. Eng. Jpn.* **1983**, *16*, 470.
(24) Gregg, S. J.; Sing, K. S. W. *Adsorption Surface Area and Porosity*; Academic Press: London, 1982.

Table 1. Variables in the Synthesis of the Samples

sample	Al/Ga[a]	OH/ (Al + Ga)[a]	pH[b]	Al^{3+c}	Ga^{3+c}	Al/Ga[d]	pill/g 10^{20e}
A	12/1	1.50	2.3	3.0	0.2	15.0	0.49
B	12/1	1.75	3.6	6.8	0.5	13.6	1.13
C	12/1	2.00	3.7	8.0	0.6	13.3	1.33
D	12/1	2.25	3.8	7.3	0.6	12.2	1.22
E	12/1	2.50	4.3	7.5	0.6	12.5	1.25
F	3/1	2.00	4.0	1.6	3.9	0.4	0.85
G		2.00	3.8	9.7			1.50

[a] Molar ratios used in the preparation of the oligomers. [b] pH of the oligomer solution after ageing. [c] Amount of cation incorporated (mequiv/g) into the pillaring products. [d] Ratio of cations incorporated. [e] Number of pillars per gram of clay.

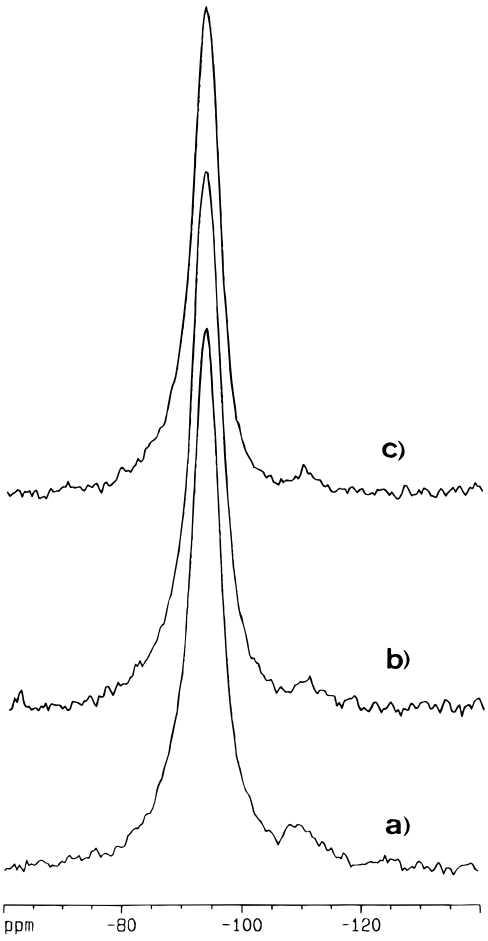

Figure 1. ^{29}Si MAS spectra: (a) sodium montmorillonite; (b) sample G pillared with ($AlAl_{12}$); and (c) sample C pillared with ($GaAl_{12}$).

previously published results[18] corresponding to a pillared sample with a molar ratio of Al/Ga = 3 in the initial oligomer, while sample G represents a pillared clay with only aluminum pillars ($AlAl_{12}$).

MAS NMR Spectra. *^{29}Si MAS NMR Spectra.* Figure 1 shows the ^{29}Si spectra obtained for the samples C and G, as well as that of montmorillonite-Na. All the spectra are very similar, showing a single signal, centered at 93.8 ppm with a width at half-height around 6 ppm. This signal is attributable to one ^{29}Si coordinated with three silica tetrahedra, Q^3(OAl), as reported in the literature[26,27] for the bidimensional framework of sheet silicates. The fact that this signal does not shift in samples C and G indicates that this bidimensional framework is maintained in the pillared materials.

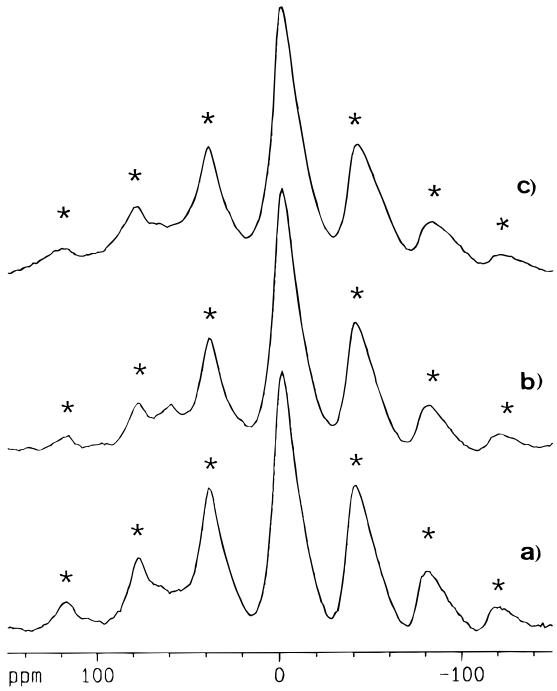

Figure 2. ^{27}Al MAS spectra: (a) sodium montmorillonite; (b) sample G pillared with ($AlAl_{12}$); and (c) sample C pillared with ($GaAl_{12}$).

^{27}Al NMR Spectra. The ^{27}Al spectra of the samples studied are included in Figure 2. That corresponding to montmorillonite-Na shows a central line near 0 ppm, with its spinning sidebands (SSB) marked with asterisks, assigned to Al^{VI} of the octahedral layer of sheet silicates.[26,27] A very weak signal around 60 ppm is hardly observable in this sample, being attributable to Al^{IV} coming from the replacement of Si by Al in the tetrahedral layer.

Sample G, with ($AlAl_{12}$) pillars, shows clearly this latter signal at 60 ppm due to the presence of tetrahedral Al in the central position of the oligomer ($AlAl_{12}$), together with the line at 0 ppm and its SSB, as in the sodium montmorillonite sample.

By contrast, in sample C, with ($GaAl_{12}$) pillars, the signal of the Al^{IV} is again hardly observable, as in the Na sample, thus indicating that there is not tetrahedral aluminum in the pillars generated in the material, due to the replacement of the tetrahedral aluminum by the Ga^{3+} cation in the central position of the oligomer ($GaAl_{12}$).

X-ray Diffraction. Figure 3 compares the evolution of the X-ray diffraction diagrams between 3 and 12° (2θ) of the samples C and G which were subjected to thermal treatment at 500 and 700 °C as well as the untreated samples. It can be seen that the untreated sample G, which is pillared only with Al, displays a d(001) peak at 18.9 Å, while the untreated sample C, which is pillared with Al−Ga, displays a peak at 19.4 Å. In the samples treated at 500 °C, the basal spacing is reduced slightly, to 17.5 and 18.1 Å, respectively. The symmetry

(25) Bradley, S. M.; Kydd, R. A.; Fyfe, C. A. *Inorg. Chem.* **1992**, *31*, 1181.

(26) Plee, D.; Borg, F.; Gatineau, L.; Fripiat, J. J. *J. Am. Chem. Soc.* **1985**, *107*, 2362.

(27) Fripiat, J. J. *Catal. Today* **1988**, *2*, 281.

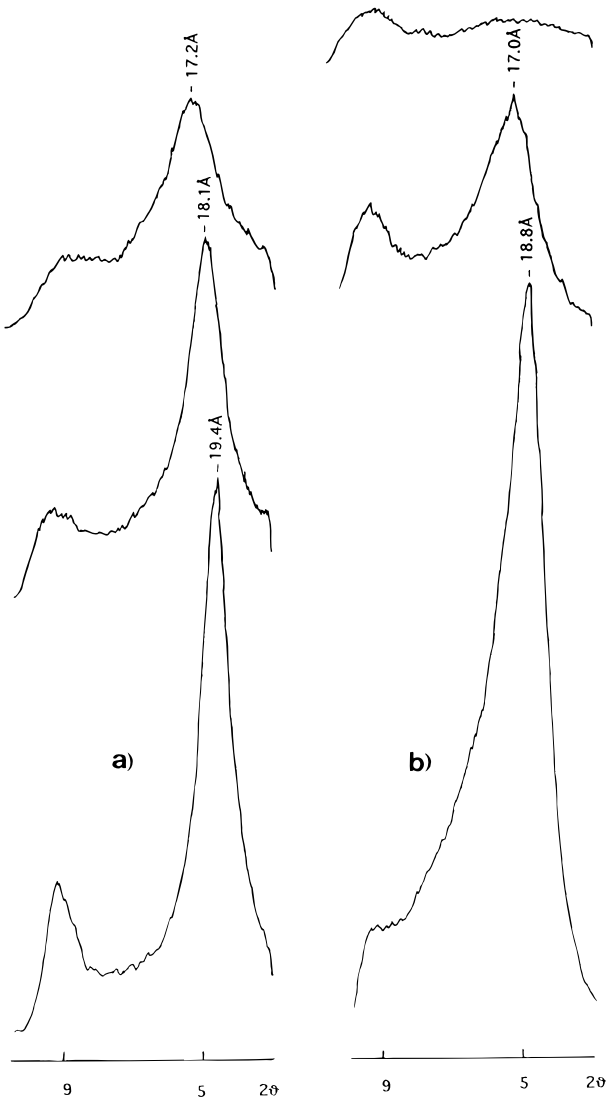

Figure 3. XRD plots at room temperature, 500, and 700 °C from bottom to top: (a) sample C; (b) sample G.

and intensity of the *d*(001) peaks confirm the existence of pillared material that is stable up to this temperature. In the samples treated at 700 °C, the basal spacing collapses for sample G, which is pillared only with Al, whereas sample C retains a peak at 17.2 Å, confirming the existence of pillared material in this sample after treatment at 700 °C.

Thermal Analysis. Figure 4 shows the thermograms of samples C and G. The thermograms clearly show two steps. Sample G presents a weight loss of 16.4% between 25 and 260 °C. This value corresponds to the water adsorbed on the external and internal surfaces. The second step, above 260 °C, indicates a mass loss (8.4%) associated with the dehydration and dehydroxylation of the $AlAl_{12}$ polyoxycation incorporated between the sheets of clay. The DTG of sample G shows the minimum of this step at 366 °C. Sample C also shows a mass loss of 15.8% in the first step (25−355 °C) while in the second step above 355 °C, there is a mass loss (5.5%) associated with the dehydration and dehydroxylation of the ($GaAl_{12}$) polyoxycation pillared between the sheets of clay. The DTG of sample C has the minimum of this step at 503 °C, which is considerably higher than that of sample G, pillared only with Al.

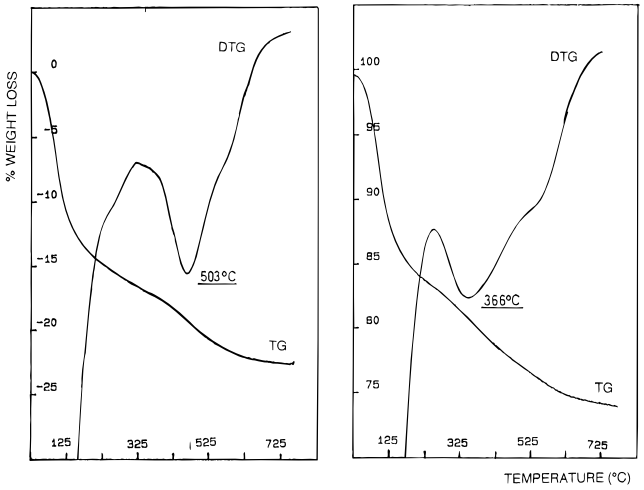

Figure 4. Thermograms of samples C, on the left, and sample G, on the right.

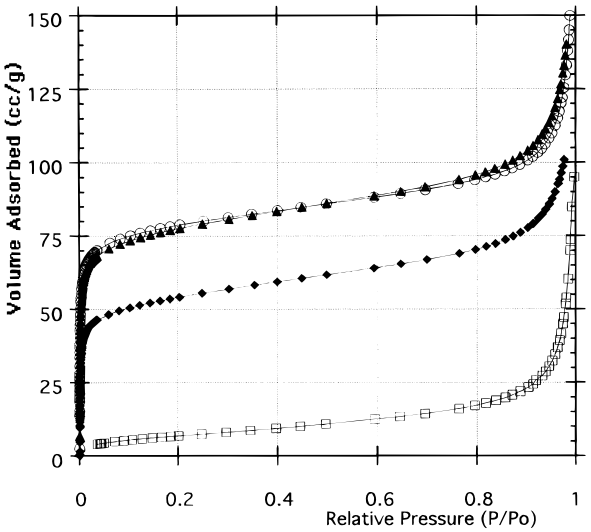

Figure 5. N_2 adsorption isotherms at room temperature and at 700 °C: ▲, sample C; ○, sample G; ◆, sample C with thermal treatment at 700 °C; □, sample G with thermal treatment at 700 °C.

Table 2. Specific Surface Area and Density of Pillars in the Samples

	S_{BET} (m^2/g)			
sample	25 °C	700 °C	%S[a]	(pillars/m^2) × 10^{17}[b]
A	290	42	14.5	1.69
B	311	191	61.4	3.63
C	292	206	70.5	4.55
D	305	177	58.0	4.00
E	324	179	55.2	3.86
G	303	25	8.3	4.95

[a] Percent of surface conservated at 700 °C. [b] Number of pillars/m^2 of surface.

Textural Analysis: Specific Surface. Figure 5 shows the N_2 isotherms at 77 K for samples C and G at room temperature and at 700 °C. These samples were selected because the rest of the samples showed parallel isotherms. In the zone with low values of P/P_0, Langmuir type I adsorption isotherms are observed, indicating the presence of micropores, whereas in the zone with high values of P/P_0, type IV isotherms are found, which correspond to mesoporous solids. Table 2 presents the values of S_{BET} of different samples at room temperature and at 700 °C, the percentage surface (%S) after thermal

Table 3. Textural Parameters of Samples C and G at Different Temperatures

	S_{BET} (m^2/g)		V_{ad} (0.98) (cm^3/g)		V_{mp} (*t*-plot) (cm^3/g)		V_{mp}[a](H−K) (cm^3/g)		V_{mp}[b](D−R) (cm^3/g)	
temp (°C)	C	G	C	G	C	G	C	G	C	G
25	292	303	0.214	0.202	0.100	0.105	0.092	0.095	0.123	0.125
500	286	223	0.203	0.187	0.090	0.074	0.091	0.071	0.121	0.090
600	254	100	0.181	0.123	0.076	0.022	0.081	0.031	0.118	0.043
700	206	26	0.162	0.081	0.065	0.000	0.062	0.004	0.096	0.012
800	34		0.140		0.000		0.008		0.014	

[a] Volume of micropore deduced from Horvath−Kawazoe method. [b] Volume of micropore deduced from Dubinin−Radushkevich method.

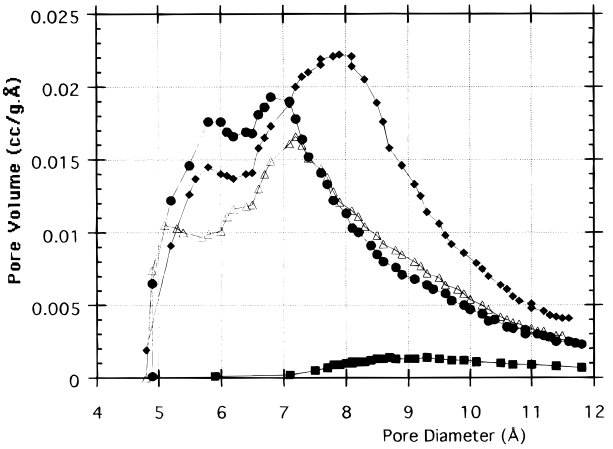

Figure 6. Micropore size distributions of ◆, sample C and ●, sample G with thermal treatment at 500 °C; △, sample C and ■, sample G with thermal treatment at 700 °C.

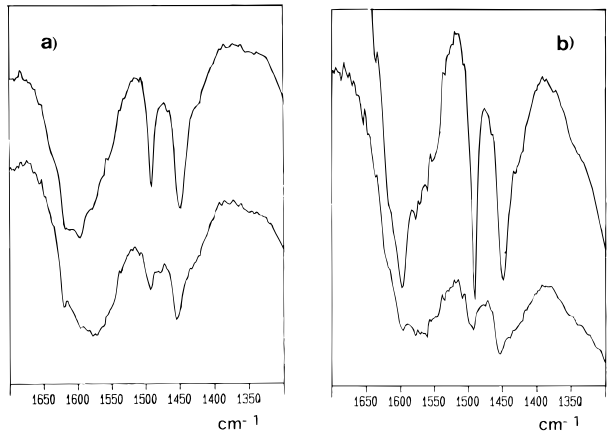

Figure 7. IR spectra of adsorbed pyridine: (a) sample C and (b) sample G, degassing at 200 °C (top) and 400 °C (bottom).

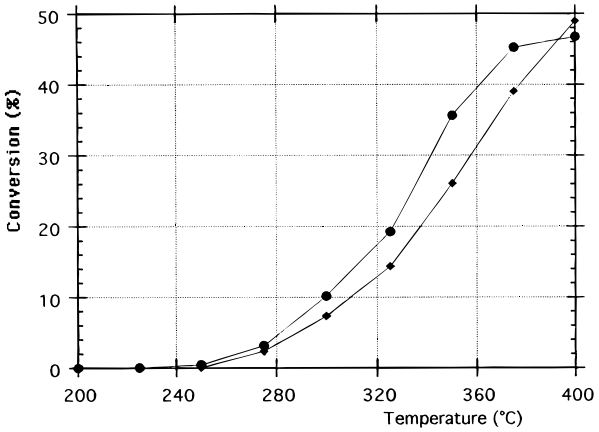

Figure 8. Conversion of *n*-heptane vs reaction temperature: ◆, sample C; ●, sample G.

treatment at 700 °C for 2 h in air, and the number of pillars/m^2 of surface.

It can be seen from the data compiled in Tables 1 and 2 that sample C, whose molar ratio is OH/Ga + Al = 2.0, is the one which displays the best results. This sample has greater stability of the specific surface area of 700 °C and more pillars per m^2 and also per gram. Therefore, from now on we will take sample C ($GaAl_{12}$) as a reference in the comparative study with sample G, which is pillared with the keggin ion, ($AlAl_{12}$).

Textural Analysis: Microporosity. The microporosity generated by the pillaring process had been analyzed, especially in samples C and G. Table 3 shows the values of the micropore volume of the samples at room temperature and after thermal treatment at 500, 600, 700, and 800 °C. It can be seen that, parallel to the decrease in the S_{BET} or V_{ad} ($P/P_0 = 0.98$), there is a decrease in the micropore volume with the temperature of the thermal treatment, independently of which one of the previously mentioned methods is used to measure it. However, there is a significant difference between the behaviors of the two samples. The microporosity of sample G falls sharply above 500 °C, while in sample C the decrease occurs at temperatures above 700 °C. Indeed, at 700 °C sample C still retains 65% of its initial micropore volume. Figure 6 shows the distribution of micropore volume as a function of pore diameter, as deduced from the H−K method.

Acidity of Samples by Pyridine Adsorption Using IR Spectroscopy. Figure 7 presents the infrared spectra in the region 1700−1300 cm^{-1} of pyridine adsorbed on samples C and G. The samples treated at 100 °C after pyridine adsorption exhibit the bands at 1448 and at 1598 cm^{-1}, which are assigned to Lewis centers, and a band at 1490 cm^{-1} attributed to both Lewis and Brönsted acid sites.[28] There is also a small band at 1550 cm^{-1} and a shoulder at 1638 cm^{-1} due to Brönsted acid sites. Sample G, with only ($AlAl_{12}$) pillars, shows a higher intensity in the bands corresponding to both Brönsted and Lewis acid centers, which is attributed to the larger number of pillars per gram of material (Table 1). When the desorption temperature of pyridine is increased, the band assigned to Lewis centers weakens faster in sample G than in sample C, indicating greater strength of the Lewis centers in sample C. This makes the B/L ratio smaller for sample C.

Catalytic Activity. In Figure 8 the conversion for samples C and G is plotted as a function of the reaction temperature. Sample G shows a greater conversion than sample C for most of the temperature range, although the conversion of sample C increases continuously and finally surpasses G at the highest temperatures. Figure 9 shows the selectivity in isomerization products vs total conversion. The straight line in this

(28) Parry, E. R. *J. Catal.* **1963**, *2*, 371.

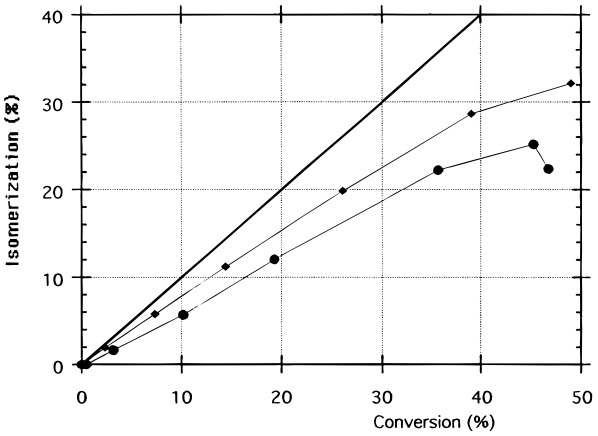

Figure 9. Yield of isomerization products vs conversion of *n*-heptane: ◆, sample C; ●, sample G.

figure corresponds to the situation where all the products obtained are isomerization products (100% selectivity). It can be seen clearly that sample C with $GaAl_{12}$ pillars shows a shift in selectivity towards isomerization. This shift becomes much stronger as the percentage of conversion or temperature increases.

Discussion

Samples A−E (Table 1) show a ratio of Al/Ga incorporated close to 12/1, which is the same proportion as in the starting solution used for the preparation of the oligomer ($GaAl_{12}$). This contrasts with the molar ratio of Al/Ga incorporated in sample F, where the initial ratio of the starting solution was 3/1. It can be seen that the greatest incorporation of Al + Ga and the highest pillaring density were obtained with an oligomeric solution having a pH of 3.7 and a molar ratio of OH/(Al + Ga) = 2.0. These are therefore the best conditions for obtaining the mixed polyoxycation ($GaAl_{12}$) and, in fact, are the same conditions used for obtaining the ($AlAl_{12}$) polyoxycation,[18] i.e., sample G.

The presence of this mixed polyoxycation ($GaAl_{12}$) is confirmed by the NMR spectra (Figure 2). The substitution of Ga for Al in the tetrahedral position of the keggin ion in sample C is indicated by the disappearance of the signal corresponding to tetrahedral Al^{IV}, which is present in sample G. In agreement with these results, it can be seen in the X-ray diffractograms (Figure 3) that the peak corresponding to the basal spacing *d*(001) at 18.9 Å in sample G disappears at 700 °C, which is due to the collapse of the structure. By contrast, sample C retains a basal spacing with a value of 17.2 Å at this temperature.

The thermal analysis (Figure 4) shows that the thermal decomposition of the polyoxycation of sample C takes place at a higher temperature, justifying the higher thermal stability of the basal spacing. The higher stability of mixed polyoxycations are compared to the keggin ion can be explained in the following way. When the Al^{IV} (radius Al^{3+} = 0.50 Å) in central tetrahedral position in the keggin ion is replaced by a Ga^{3+} cation (radius Ga^{3+} = 0.62 Å) in the mixed polyoxycation ($GaAl_{12}$) (Figure 10), the 12 octahedral aluminums surrounding the Ga^{3+} cation present a spatial distribution with less stearic impediment.

In the textural study by means of N_2 adsorption isotherms (Table 2) it was found that pillaring with

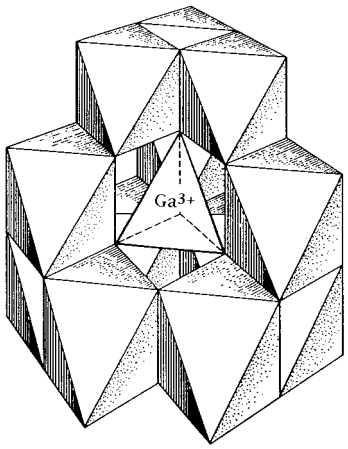

Figure 10. Schematic structure of the $[AlO_4Al_{12}(OH)_{24}(H_2O)_{12}]^{7+}$ and $[GaO_4Al_{12}(OH)_{24}(H_2O)_{12}]^{7+}$ polyoxycations with the central tetrahedral position surrounded by 12 octahedral aluminums.

$GaAl_{12}$, i.e., samples B−E increased the specific surface area up to nearly 300 m^2/g, as in sample G, which was pillared with ($AlAl_{12}$). However, when the samples were heat-treated at 700 °C, samples B−E retained a high percentage of their specific surface area, especially sample C (71%), whereas sample G collapsed, with its surface area decreasing dramatically to 25 m^2/g. The higher stability in surface area sample C is probably related to the higher number of pillars/m^2. Sample A does not show the same stability as samples B−E due to the significantly smaller number of pillars/m^2. The lower stability of sample G, on the other hand, can be explained by the nature of the pillars, which are made up of keggin ions ($AlAl_{12}$).

The different evolution of microporosity with temperature of samples C and G must be attributed to a higher thermal stability of the mixed pillars ($GaAl_{12}$) which withstand temperatures up to 700 °C. The maximum diameter observed in the distribution of micropore volume versus diameter (Figure 6) is in agreement with the basal spacing deduced by X-ray diffraction, taking in account the fact that this value is the sum of the interlayer spacing occupied by the pillars and the thickness of the montmorillonite clay layer (9.6 Å).

The incorporation of pillars produces an increase in the acidity of both samples C and G, especially of Lewis acid centers, due to the presence of aluminum cations in the pillars. This is also in agreement with the studies made by Bradley and Kydd.[29] The fact that sample C, pillared with ($GaAl_{12}$), shows less destruction of the bands corresponding to these Lewis acid centers in the thermic desorption of pyridine demonstrates that the Lewis centers are stronger in sample C. This may well be due to the higher electronegativity of gallium (EN = 1.8) as compared to that of aluminium (EN = 1.5), which would diminish the electronic density associated to Lewis centers constituted by Al^{VI} (Al^{VI}−O−Ga^{IV}−).

In the hydroisomerization and hydrocracking of *n*-heptane, the sample with ($GaAl_{12}$) pillars showed a lower conversion throughout the temperature range than the sample with ($AlAl_{12}$) pillars. This can be attributed to the smaller number of acid centers, resulting from the lower number of pillars/m^2. The fact that

(29) Bradley, S. M.; Kydd, R. A. *J. Catal.* **1993**, *141*, 239.

conversion continues to increase at higher temperatures in sample C seems to be related to the higher thermal stability of the pillars and acid centers. It seems reasonable to suggest that the higher selectivity of isomerization of sample C would be due to the lower ratio of B/L centers.

Conclusions

The optimum conditions for the preparation of the polyoxycation $[GaO_4Al_{12}(OH)_{24}(H_2O)_{12}]^{7+}$ are the following: pH = 3.7; molar ratio of $OH/Al^{3+} + Ga^{3+} = 2.0$; and molar ratio of $Al^{3+}/Ga^{3+} = 12/1$. The presence of the ($GaAl_{12}$) polyoxycation in the obtained material has been verified by means of NMR studies.

The characteristics of the material obtained with the ($GaAl_{12}$) polyoxycation have been compared with those of the same montmorillonite pillared with the $[AlO_4Al_{12}(OH)_{24}(H_2O)_{12}]^{7+}$ ion. It was found that the mixed pillars have a higher thermal stability, resulting in greater thermal stability of the structure. The material obtained with the ($GaAl_{12}$) polyoxycation also retains 65% of its generated microporosity up to 700 °C and has a higher stability in the number and strength of Lewis acid centers of its pillars. This may account for the higher catalytic conversion at high temperatures and greater selectivity for isomerization.

Acknowledgment. We wish to acknowledge the financial support of this work provided by the Comisión Investigación Científica y Técnica (CICYT) under Projects MAT92/0940 and MAT95/0143 and also the expert assistance of Dr. R. Alvero and the Servicio de Resonancia Magnética Nuclear of the Universidad de Sevilla.

CM950225M